

## Parallel Generation of Quadripartite Cluster Entanglement in the Optical Frequency Comb

Matthew Pysher,<sup>1</sup> Yoshichika Miwa,<sup>2</sup> Reihaneh Shahrokhshahi,<sup>1</sup> Russell Bloomer,<sup>1</sup> and Olivier Pfister<sup>1,\*</sup>

<sup>1</sup>*Department of Physics, University of Virginia, Charlottesville, Virginia 22903, USA*

<sup>2</sup>*Department of Applied Physics, School of Engineering, The University of Tokyo, 7-3-1 Hongo, Bunkyo-ku, Tokyo 113-8656, Japan*

(Received 28 March 2011; published 14 July 2011)

Scalability and coherence are two essential requirements for the experimental implementation of quantum information and quantum computing. Here, we report a breakthrough toward scalability: the simultaneous generation of a record 15 quadripartite entangled cluster states over 60 consecutive cavity modes ( $Q$  modes), in the optical frequency comb of a single optical parametric oscillator. The amount of observed entanglement was constant over the 60  $Q$  modes, thereby proving the intrinsic scalability of this system. The number of observable  $Q$  modes was restricted by technical limitations, and we conservatively estimate the actual number of similar clusters to be at least 3 times larger. This result paves the way to the realization of large entangled states for scalable quantum information and quantum computing.

DOI: 10.1103/PhysRevLett.107.030505

PACS numbers: 03.67.Bg, 03.65.Ud, 03.67.Mn, 42.50.Dv

*Introduction.*—The experimental implementation of quantum computing, driven by the promise of exponential speedup for tasks such as the simulation of quantum physics [1] and integer factoring [2], is a daunting challenge that requires exquisite levels of control over the quantum mechanical properties of numerous individual physical systems (quantum bits or, in this Letter, quantum modes or  $Q$  modes). The response to this challenge spawned a wealth of experimental research efforts in widely different fields [3], striving to enable and maintain quantum-coherent temporal evolution of quantum bits while at the same time scaling up their number. Here, we demonstrate a breakthrough toward scalability: the novel, ultracompact implementation of quantum registers in the optical frequency comb (OFC) formed by the spectrum of a *single* optical parametric oscillator (OPO), thereby utilizing a capability for quantum information storage analogous to that exploited classically in FM radio or wavelength multiplexing. The classical OFC generated by ultrastable pulsed lasers has found groundbreaking uses in ultimate precision frequency measurements [4,5]. In the case of the quantum OFC, each ( $Q$ ) mode is well approximated by a quantum harmonic oscillator whose continuous-variable Hilbert space is defined by its amplitude- or phase-quadrature field observable (analogues of the position and momentum observables). There is no known fundamental impossibility to the implementation of quantum computing with  $Q$  modes [6–8], even though the implementation of quantum error correction appears likely to require Hilbert-space discretization [9,10]. A method to create a frequency-degenerate  $N$ - $Q$  mode register was proposed, by use of  $N$  OPOs and a  $2N$ -port interferometer [11], and demonstrated [12,13] for 3 and 4  $Q$  modes. However, it was also shown that a square-grid continuous-variable cluster state of arbitrary size, suitable for universal one-way quantum computing [8,14], can be generated in the OFC of a single OPO [15,16]. In this work,

we achieved the first step toward this goal: the parallel generation of 15 quantum computing registers, each comprising 4  $Q$  modes in a quadripartite cluster state, in the quantum OFC of a single OPO. Requirements for the generation of larger entangled states include the experimental progress made in this work, along with a richer pump spectrum and a more tailored nonlinear interaction [15,16].

*Experimental method.*—The quantum OFC was generated by a bow-tie ring OPO containing two  $x$ -cut KTiOPO<sub>4</sub> (KTP) nonlinear crystals, of 10 mm length, and rotated by 90° from each other about the  $x$  axis. This ensured the perfect overlap of the respective OFCs of orthogonal linear polarizations  $y$  and  $z$ . One crystal was not phase-matched. The other was periodically poled with two distinct periods: 9  $\mu\text{m}$  over a 3 mm length and 458  $\mu\text{m}$  over 7 mm. The former quasi-phase-matched the  $zzz$  parametric down-conversion, where the first letter denotes the polarization of the pump field at frequency  $2\omega_0$  and the other letters denote the polarization of the  $n$ th signal field pair at  $\omega_{\pm n} = \omega_0 \pm (n - 1/2)\Delta$ , with  $\Delta = 945.66$  MHz the free spectral range of the OPO cavity. The latter period quasi-phase-matched the  $zyz$  and  $yyz$  interactions simultaneously (dispersion was negligible for our values of  $n$ ). The pump polarization was carefully adjusted in the ( $yz$ ) plane, by using OPO characterization by resonant second harmonic generation [17], to yield the Hamiltonian [18]

$$H = i\hbar\kappa \sum_n (a_{-n,z}^\dagger a_{n,z}^\dagger + a_{-n,y}^\dagger a_{n,z}^\dagger + a_{-n,z}^\dagger a_{n,y}^\dagger) + \text{H.c.}, \quad (1)$$

where  $a_{j,k}^\dagger$  is the creation operator of the  $k$ -polarized  $Q$  mode of frequency  $\omega_j$ . This Hamiltonian entangles the OFC as depicted in Fig. 1 and proven by the solutions of the Heisenberg equations for the  $n$ th  $Q$  mode quartet:

$$Q_+ = \{[Q_{-n,y} - Q_{n,y}] + \Phi[Q_{-n,z} - Q_{n,z}]\}e^{-r\Phi}, \quad (2)$$

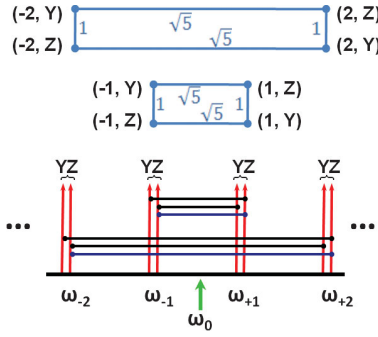


FIG. 1 (color). Principle of the experiment. The OFC of a single OPO is made polarization-degenerate by using a cavity with 2 identical crystals rotated  $90^\circ$  from each other in the polarization plane. One crystal simultaneously phase-matches the  $zzz$ ,  $yzz$ , and  $yyz$  nonlinear interactions (bottom). This creates square weighted cluster states (top, in blue) [18].

$$P_+ = \{[P_{-n,y} + P_{n,y}] + \Phi[P_{-n,z} + P_{n,z}]\}e^{-r\Phi}, \quad (3)$$

$$Q_- = \{\Phi[Q_{-n,y} + Q_{n,y}] - [Q_{-n,z} + Q_{n,z}]\}e^{-(r/\Phi)}, \quad (4)$$

$$P_- = \{\Phi[P_{-n,y} - P_{n,y}] - [P_{-n,z} - P_{n,z}]\}e^{-(r/\Phi)}, \quad (5)$$

where  $Q = a + a^\dagger$  and  $P = i(a^\dagger - a)$  are the amplitude and phase quadratures, respectively,  $r$  is the squeezing parameter, and  $\Phi = (\sqrt{5} + 1)/2$ , which is the golden ratio. These four squeezed (quantum-noise-reduced) field quadratures coincide, to local quadrature phase shifts left, with the nullifiers (entanglement witnesses) of a weighted square cluster state [18] (Fig. 1) in the (unphysical) limit of infinite squeezing, where the cluster state is a zero-eigenvalue eigenstate of the nullifiers. The exponentiated nullifiers are thus the stabilizers of the entangled state [19] (in contrast to the  $Q$  bit case, weighted  $Q$  mode cluster states are stabilizer states [20]). For a pure state, observing the squeezing of a nullifier suffices to prove that the state has been prepared into a stabilizer state. For a statistical mixture, the situation is more complicated, but one can still use the van Loock–Furusawa criteria [21] to prove quadripartite nonseparability. We experimentally demonstrated both.

The setup is described in Fig. 2. The OPO, pumped at 532 nm by a frequency-doubled, ultrastable continuous-wave Nd:YAG laser (Innolight Diabolo), consisted of a cavity with low-loss mirrors and a 5% output coupler. The quantum OFC was separated into its orthogonal polarizations, and quadrature combinations, e.g.,  $Q_{-n,y} \pm Q_{n,y}$  in Eqs. (2)–(5), were measured by two-tone balanced homodyne detection with local oscillator (LO) fields at  $\omega_{\pm n}$ . The LO originated from another Nd:YAG laser (Lightwave Electronics) which was phase-locked to the 1064 nm pump laser before it was frequency-doubled [17]. The LO laser frequency could therefore coincide with  $\omega_0$  (Fig. 3) or differ from it for experimental verifications (Fig. 4). The  $\omega_{\pm n}$  frequencies were then generated

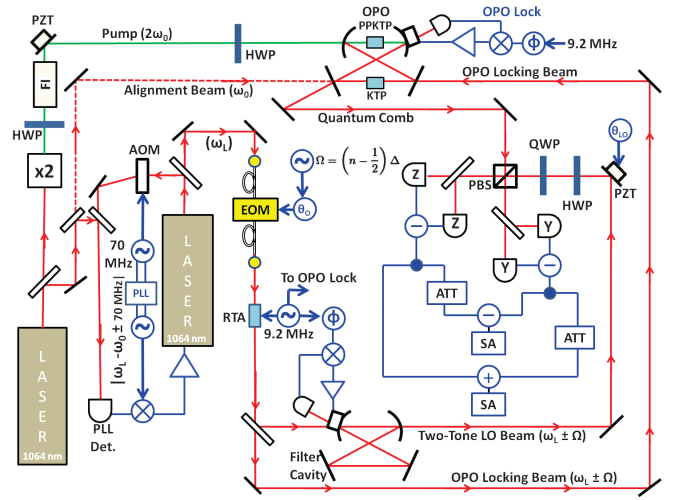


FIG. 2 (color). Experimental setup. HWP, half wave plate; QWP, quarter wave plate; FI, Faraday isolator; PZT, piezoelectric transducer; PLL, phase-lock loop; AOM, acousto-optic modulator; EOM, waveguide electro-optic modulator; KTP, KTiOPO<sub>4</sub>; RTA, RbTiAsO<sub>4</sub> EOM; PBS, polarizing beam splitter; ATT, rf attenuator; SA, spectrum analyzer.

by phase electro-optic modulation (EOM) and subsequent bandpass filtering by an optical cavity of the same free spectral range as the OPO, in order to remove the carrier and second harmonics. The homodyne visibilities were 97% for the  $y$  polarization and 96% for  $z$ . Finally, the homodyne photocurrents from 95% efficient InGaAs photodiodes (JDSU ETX500T) were preamplified and combined by rf splitters and attenuators in order to yield the variance of nullifiers (2) and (5), observed synchronously on two spectrum analyzers while the LO optical path  $\theta_{LO}$  was scanned. The measured observables can be expressed in terms of generalized quadratures  $A(\theta) = ae^{-i\theta} + a^\dagger e^{i\theta}$  as

$$A_{\pm}(\theta) = \{[A_{-n,y}(\theta) \mp A_{n,y}(-\theta)] \pm \Phi^{\pm 1}[A_{-n,z}(\theta) \mp A_{n,z}(-\theta)]\}e^{-r\Phi^{\pm 1}}, \quad (6)$$

where phase values  $\theta = 0$  and  $\pi/2$  yield amplitude and phase quadratures, respectively. Note that the squeezing is independent of  $\theta$ . Because we use two-tone homodyne detection,  $\theta$  is a function of  $\theta_{LO}$  and of the EOM phase  $\theta_0$  (Fig. 2), and the different nullifiers Eqs. (2)–(5) are obtained for the respective values  $(\theta_{LO}, \theta_0) = (0, 0)$ ;  $(0, \pi/2)$ ;  $(\pi/2, \pi/2)$ ;  $(\pi/2, 0)$ , modulo  $\pi$ . Additional checks were made by using LO polarization [17].

*Results.*—Fifteen sets of 4  $Q$  modes were measured for  $n = 1$ –15. The measurement results are displayed in Fig. 3. As can clearly be seen, the level of squeezing is constant over the whole set of 15 observed clusters, which establishes scalability in the OFC. Moreover, the maximum value of  $n = 15$  was not fixed by the quantum state preparation process but by measurement limitations: the 14 GHz bandwidth limit of the EOM. The state preparation bandwidth is given by the phase-matching bandwidths of the

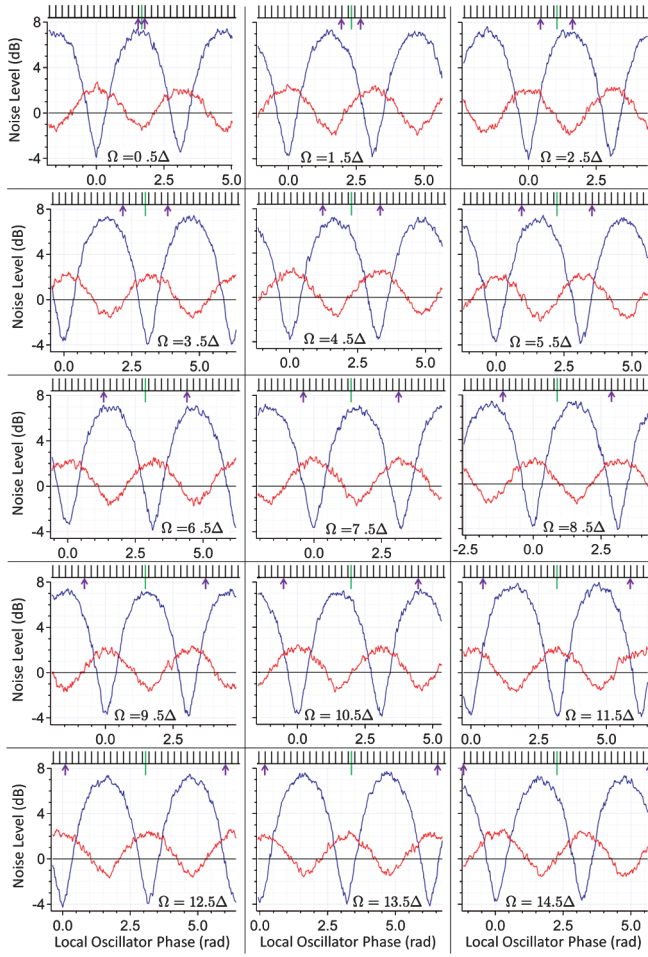


FIG. 3 (color). Scaling quadripartite entanglement in the optical frequency comb of a single OPO: nullifier variance  $\Delta A_{\pm}[\theta(\theta_{LO})]^2$ , relative to the vacuum noise, versus the LO phase  $\theta_{LO}$ . Note that the squeezing depends on  $\theta_{LO}$  but not on  $\theta$  [17]. Single-sweep measurements were taken at 1.25 MHz frequency; RBW: 30 kHz; VBW: 30 Hz. The  $Q$  modes (black lines) measured are marked by the LO sidebands (purple arrows). The green line references half the pump frequency.

nonlinear interactions. We calculated these for the  $zzz$  and  $yzy$  processes, respectively, to be 616 and 47 GHz at 99% of the maximum. This indicates that a 1% squeezing decrease occurs for the  $yzy$  interaction at 47 GHz (a 10% decrease at 153 GHz). This is too weak an effect to be observed at our current squeezing level, and cluster states  $n = 16, \dots, 47$  should therefore be identical to the ones measured in Fig. 3. We therefore expect that 3–10 times as many cluster states were generated than the 15 that were accessible with our setup. We can also flattop shape the phase-matching curve [22] in order to optimize scalability.

Phase-locking our two 1064 nm lasers to each other allowed us to make the crucial checks necessary to test the validity of our experimental results, in particular, of our two-tone homodyne detection. These checks consisted of using a single LO sideband, placing the LO sidebands at uncorrelated frequencies, and detuning the pump frequency from our quantum OFC. Figure 4 shows typical

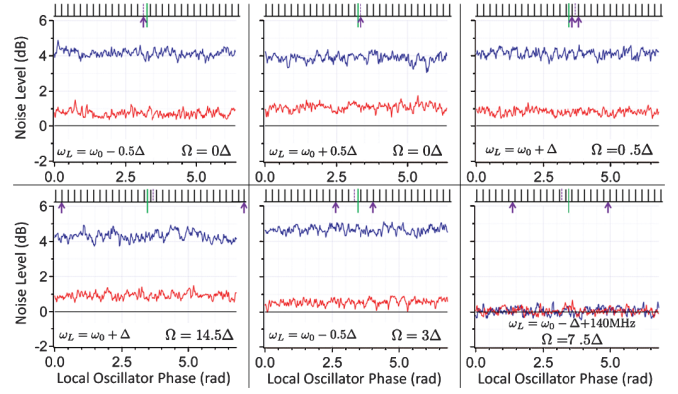


FIG. 4 (color). Detection and entanglement checks. As in Fig. 3, the plots display nullifier variance measurement relative to the vacuum noise versus the LO phase  $\theta_{LO}$ . Top row, left and center: Single-sideband detection displays no single-mode squeezing in the OPO comb, in any quadrature. Top row, right, and bottom row, left and center: LO sidebands coincide with uncorrelated comb lines, in any quadrature, which yields no multimode squeezing whatsoever, again no matter the LO phase used. Bottom row, right: OPO pump detuned from the comb ( $2\omega_0 \neq \omega_{-n} + \omega_n$ ), which makes the nonlinear interaction singly (instead of doubly) resonant and yields negligible squeezing. Notations and legends are as in Fig. 3. The dashed purple line references the phase-locked laser’s frequency.

results, which all agree with theoretical predictions [17] and clearly show no quantum correlations whatsoever, in stark contrast to the nullifier squeezing signals of Fig. 3. An essential point here is that all these verification results were insensitive to the LO phase, unlike the nullifier measurements.

We finally address pure state preparation. The fact that the antisqueezing magnitude is larger than the squeezing one points to the existence of losses and additional classical noise (from the pump laser) and, therefore, to the creation of a statistical mixture rather than a pure state. This can be alleviated by filtering the pump field with a “mode-cleaner” cavity, which we did not do so as to maximize the pump power and hence the amount of squeezing. Nullifier squeezing is enough to claim entanglement if the state is pure. In order to ascertain

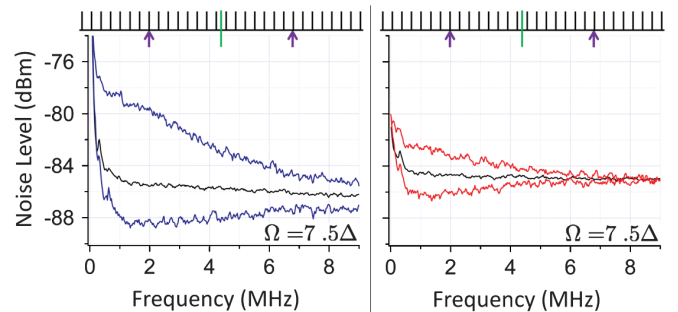


FIG. 5 (color). Squeezing spectra for  $A_+$  (left) and  $A_-$  (right). The squeezed trace on the left was recorded simultaneously with the antisqueezed trace on the right, for  $\theta_{LO} = \pi/2$ , and vice versa, for  $\theta_{LO} = 0$ , as with measurements in Figs. 3 and 4.

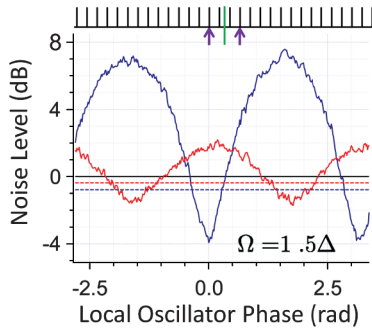


FIG. 6 (color). Variances  $(\Delta A_+)^2$  (blue) and  $(\Delta A_-)^2$  (red) with measurement gains set to 0.3 in lieu of  $1/\Phi = 0.618$ . (The van Loock–Furusawa criterion allows us to deviate from nullifier measurements to find the optimum gain values for maximum violation.) The dashed lines indicate the sub-vacuum-noise violation levels required to prove inseparability.

this, we measured the squeezing spectra of  $A_{\pm}$  at the optimum phases (Fig. 5). As can be seen, the state is pure for measurement frequencies above 5 MHz [17], which validates our cluster-state preparation claim.

In the case of a mixture, as in the case of our 1.25 MHz measurement frequency (which yields more squeezing), one can use the van Loock–Furusawa separability criterion [21] in order to show that no  $Q$  mode can be placed in a factorized density operator of its own. A detailed analysis [17] led to five van Loock–Furusawa inequalities that must all be experimentally violated. While some of these inequalities have bounds at the vacuum level and are trivially violated by mere nonzero squeezing, others have bounds below the vacuum noise and therefore present higher violation thresholds. Figure 6 displays experimental results for the two most difficult such cases, which were clearly violated, thereby proving quadripartite entanglement even in a mixed state.

*Conclusion.*—We demonstrated that the optical frequency comb of a single optical parametric oscillator lives up to its promise as an extremely scalable system for quantum information. We simultaneously generated a record number of quadripartite cluster states, in a record number of  $Q$  modes, all equally entangled. The quantum comb was read by two-tone homodyne detection. Even though the size of the entangled states themselves is not a record, compared to the 14-ion Greenberger–Horne–Zeilinger state [23], we demonstrated stringent state preparation requirements for cluster states, a universal quantum computing resource. A practical quantum computer will require an increase in both the number of entangled modes and the amount of squeezing. However, the projective measurements required for one-way quantum computing can already be performed on the clusters that we generated [24]. Variants of our setup will allow the generation of multiple cube graphs [18] and a scalable quantum wire and square-grid lattice [15,16].

This work was supported by U.S. National Science Foundation Grants No. PHY-0855632 and

No. PHY-0960047. Y.M. was supported by G-COE commissioned by the MEXT of Japan. We thank Nicolas Menicucci, Steven Flammia, Jens Eisert, and Géza Giedke for useful discussions.

\*opfister@virginia.edu

- [1] R. P. Feynman, *Int. J. Theor. Phys.* **21**, 467 (1982).
- [2] P. W. Shor, in *Proceedings of the 35th Annual Symposium on Foundations of Computer Science*, edited by S. Goldwasser (IEEE, Los Alamitos, CA, 1994), pp. 124–134.
- [3] T. D. Ladd, F. Jelezko, R. Laflamme, Y. Nakamura, C. Monroe, and J. L. O’Brien, *Nature (London)* **464**, 45 (2010).
- [4] T. W. Hänsch, *Rev. Mod. Phys.* **78**, 1297 (2006).
- [5] J. L. Hall, *Rev. Mod. Phys.* **78**, 1279 (2006).
- [6] S. Lloyd and S. L. Braunstein, *Phys. Rev. Lett.* **82**, 1784 (1999).
- [7] S. D. Bartlett, B. C. Sanders, S. L. Braunstein, and K. Nemoto, *Phys. Rev. Lett.* **88**, 097904 (2002).
- [8] N. C. Menicucci, P. van Loock, M. Gu, C. Weedbrook, T. C. Ralph, and M. A. Nielsen, *Phys. Rev. Lett.* **97**, 110501 (2006).
- [9] J. Niset, J. Fiurášek, and N. J. Cerf, *Phys. Rev. Lett.* **102**, 120501 (2009).
- [10] M. Ohliger, K. Kieling, and J. Eisert, *Phys. Rev. A* **82**, 042336 (2010).
- [11] P. van Loock and S. Braunstein, *Phys. Rev. Lett.* **84**, 3482 (2000).
- [12] T. Aoki, N. Takei, H. Yonezawa, K. Wakui, T. Hiraoka, A. Furusawa, and P. van Loock, *Phys. Rev. Lett.* **91**, 080404 (2003).
- [13] J. Jing, J. Zhang, Y. Yan, F. Zhao, C. Xie, and K. Peng, *Phys. Rev. Lett.* **90**, 167903 (2003).
- [14] R. Raussendorf and H. J. Briegel, *Phys. Rev. Lett.* **86**, 5188 (2001).
- [15] N. C. Menicucci, S. T. Flammia, and O. Pfister, *Phys. Rev. Lett.* **101**, 130501 (2008).
- [16] S. T. Flammia, N. C. Menicucci, and O. Pfister, *J. Phys. B* **42**, 114009 (2009).
- [17] See Supplemental Material at <http://link.aps.org/supplemental/10.1103/PhysRevLett.107.030505> for more information.
- [18] H. Zaidi, N. C. Menicucci, S. T. Flammia, R. Bloomer, M. Pysker, and O. Pfister, *Laser Phys.* **18**, 659 (2008), arXiv:0710.4980v3 (revised version).
- [19] M. Gu, C. Weedbrook, N. C. Menicucci, T. C. Ralph, and P. van Loock, *Phys. Rev. A* **79**, 062318 (2009).
- [20] N. C. Menicucci, S. T. Flammia, and P. van Loock, *Phys. Rev. A* **83**, 042335 (2011).
- [21] P. van Loock and A. Furusawa, *Phys. Rev. A* **67**, 052315 (2003).
- [22] M. M. Fejer, G. A. Magel, D. H. Jundt, and R. L. Byer, *IEEE J. Quantum Electron.* **28**, 2631 (1992).
- [23] T. Monz, P. Schindler, J. T. Barreiro, M. Chwalla, D. Nigg, W. A. Coish, M. Harlander, W. Hänsel, M. Hennrich, and R. Blatt, *Phys. Rev. Lett.* **106**, 130506 (2011).
- [24] Y. Miwa, R. Ukai, J.-i. Yoshikawa, R. Filip, P. van Loock, and A. Furusawa, *Phys. Rev. A* **82**, 032305 (2010).